Preprints of the 21st IFAC World Congress (Virtual)
Berlin, Germany, July 12-17, 2020

Working Distance-Based Feedforward Control of the Weld Bead Height in Directed Energy Deposition

Johann Stoppok * **David Dillkötter** * **Magnus Thiele** *
Cemal Esen * **Sebastian Leonow** * **Martin Mönnigmann** *

* *Department of Mechanical Engineering, Ruhr-Universität Bochum, 44801 Bochum, Germany (email: johann.stoppok@rub.de, david.dillkoetter@rub.de, thiele@lat.rub.de, esen@lat.rub.de and martin.moennigmann@rub.de).*

Abstract: Due to large temperature gradients and high thermal conductivities, additive manufacturing processes for metals have challenging dynamics. A high process reliability and repeatability hinges upon the base layer control of the melt pool and the resulting weld bead geometry. The material feed rate has proven to be an appropriate manipulated variable for weld bead height control, but it can only be varied slowly and is subject to deadtimes. We propose to use the distance of the process head to the build surface (the working distance) as an alternative manipulated variable. We derive a simple nonlinear dynamic model that captures the effect of the working distance on the weld bead height. We show scanning velocity fluctuations, which can be treated as known disturbances, can be compensated with working distance feedforward control. We apply the proposed controller to a real DED process and demonstrate working distance control is an alternative to material feed rate control.

Keywords: additive manufacturing, directed energy deposition, process control, metal processing, manufacturing plant control

1. INTRODUCTION

Directed energy deposition (DED) is a common approach to additive manufacturing with metallic materials. In a typical setup, a laser is focused on a build surface to create a melt pool, and material is added by feeding wire or powder to this pool. Upon moving the laser and the feeding mechanism across the build surface, a weld bead can be generated (see Figure 1 for a sketch). Layers of material

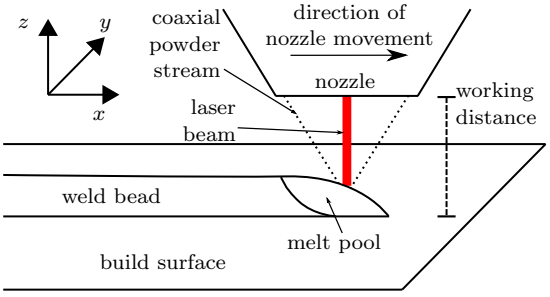

Fig. 1. Sketch of a DED processing head with laser source, coaxial powder feeding nozzle, and resulting weld bead.

and 3D structures can be built up in the same fashion as with 3D printers that use fused plastic filaments.

In order for a DED process to be reliable, it is crucial to control the geometry of the weld beads, specifically the weld bead width and weld bead height. The manipulated variables available for control are the laser power, the material feed rate, the distance of the processing head to the build surface in z-direction, and the scanning velocity, i.e., the relative velocity of the processing head to the build surface in the (x, y)-plane.

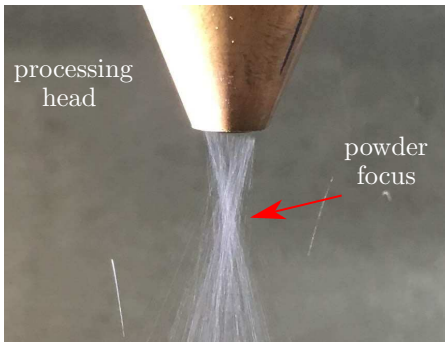

Fig. 2. Powder nozzle with the characteristic powder flow and powder focus. The distance of the lower nozzle end to the powder focus amounts to 8mm.

The weld bead height has successfully been controlled with the scanning velocity (Fathi et al., 2007). However, control of the scanning velocity is often limited, because it is typically determined by proprietary motion planners, and therefore can often only be treated as a known disturbance. Dillkötter and Mönnigmann (2019) showed the laser power can be used to compensate for changes of the weld bead width due to scanning velocity fluctuations caused by a motion planner (see also Devesse et al. (2014)). Their results are in line with those reported by De Oliveira et al.

(2005), El Cheikh et al. (2012) and Corbin et al. (2017), who found the laser power to have a strong influence on the weld bead width, but only a little effect on the weld bead height. The powder feed rate has proven to be suitable for weld bead height control (Tang et al., 2008). It can be varied fairly slowly only, however, and often is subject to deadtimes, which result from constructive details of the feeding mechanism.

We propose to use the distance of the processing head to the build surface in z-direction, which we call the working distance, as an additional manipulated variable. We show the working distance can be used for feedforward control of the weld bead height, after identification of a suitable dynamic model.

We note that the influence of the working distance has been analyzed before. Specifically, Corbin et al. (2017) described the static effect of the working distance on the weld bead height and Haley et al. (2019) analyzed its effect on the inter layer stabilizing properties. The working distance has not been used before for feedforward control of the weld bead height to the knowledge of the authors.

Section 2 presents the dynamic model, including the steps required for its identification, and introduces the feedforward controller. Section 3 reports the results obtained from applying the proposed controller to a laboratory DED process. Conclusions and an outlook are stated in Section 4.

2. FEEDFORWARD CONTROL OF THE DED-PROCESS

We show that the working distance is a useful input for weld bead height control by implementing a feedforward controller and evaluating it with a laboratory DED machine. It is the purpose of this controller to compensate variations in the weld bead height that appear whenever the processing head velocity varies. Figure 2 illustrates the central idea. It is evident from the figure that the coaxial powder nozzle focuses the powder mass flow. As a consequence, the mass flow into the melt pool can be controlled to a certain extent by changing the distance of the nozzle to the melt pool, i.e., the working distance, which we denote $d(t)$.

The melt pool has a finite size (cf. Figure 1). Depending on the magnitude of the process head velocity, the melt pool may extend into the direction of motion. This implies material may be deposited at positions that are only reached by the laser focus at a later instant. We sometimes have to shift time-series, or ignore time intervals that correspond to the melt pool extension at the current velocity, in order to ignore apparently acausal behavior.

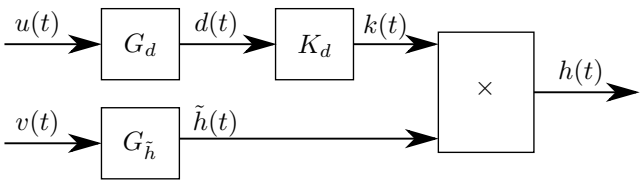

Fig. 3. Structure of the dynamic model of the system.

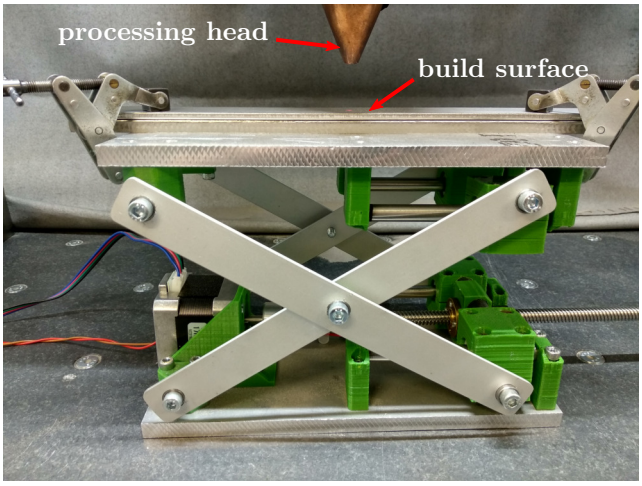

Fig. 4. Platform for fast working distance control. The pantograph is motorized with a NEMA 17 stepper motor which is controlled with a DM542A motor driver and 72 MHz STM32 microcontroller running a motionplanner.

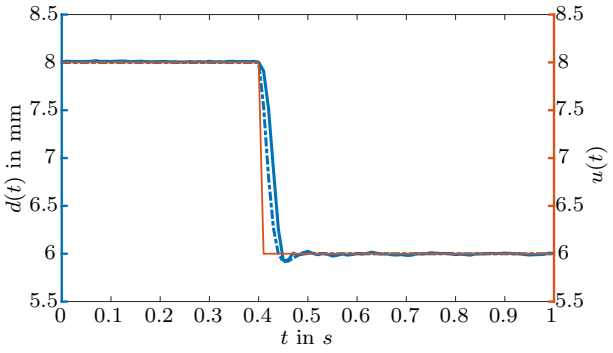

Fig. 5. Step input (red), average of three measured step responses (blue, solid) and step response of G_d (blue, dashed)

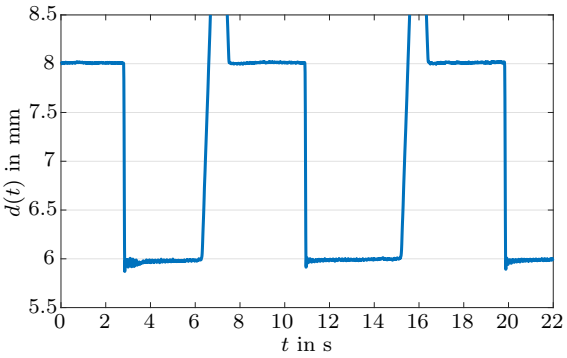

Fig. 6. Three steps in quick succession from 8 mm working distance to 6 mm working distance with homing procedure in between the steps.

We propose the model structure shown in Figure 3 and identify the required transfer functions in the subsequent subsections. Specifically, the effect of the control input $u(t)$ on the working distance $d(t)$ is modeled with the transfer function G_d identified in Section 2.1. The transfer function $G_{\tilde{h}}$, which describes the impact of the nozzle

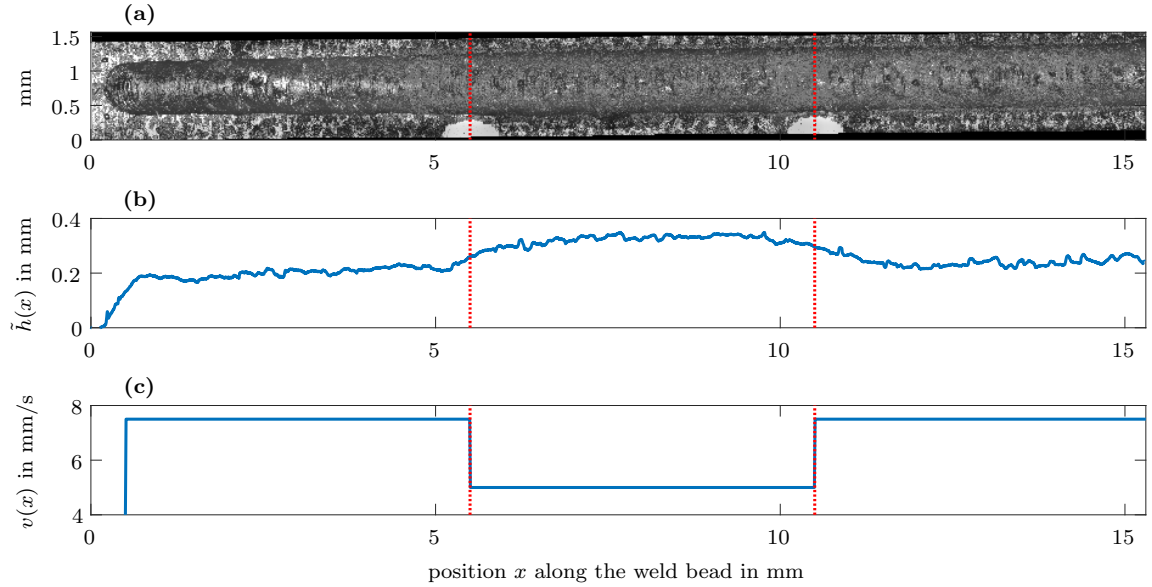

Fig. 7. Effect of the processing head velocity $v(x)$ parallel to the build surface on the weld bead height $\tilde{h}(x)$ for constant laser power (315 W), constant powder feed rate (2.4 g/min) and constant working distance (8mm). The processing head is moved along the x-axis only without restriction. The height of the weld bead shown in (b) is measured with a confocal laser scanning microscope (Keyence VK-X100) at a vertical and lateral resolution of 5 nm and 7 μm, respectively. The microscope also provides the light image shown in (a). Positions of the steps are marked with the processing laser after completing the weld and for zero powder flow here (white partial cicles in (a)) and in Figure 12.

velocity $v(t)$ on the weld bead height $\tilde{h}(t)$, is determined in Section 2.2. The efficiency factor $k(t)$, which is introduced below, depends statically on $d(t)$; the required function K_d is treated in Section 2.3. Note that the model is nonlinear due to the multiplication

$$h(t) = k(t) \cdot \tilde{h}(t). \tag{1}$$

in the rightmost block in Figure 3, but all remaining blocks are linear. After identification of all required transfer functions, the feedforward controller is introduced in Section 2.4.

2.1 Working distance dynamics (G_d)

Processing heads of typical DED manufacturing machines comprise the laser, the nozzle required for feeding the powder and measurement devices such as pyrometers. As a consequence, processings heads are heavy devices and their velocities and accelerations are often limited. The maximum acceleration of the laboratory setup in z-direction amounts to 0.1m/s^2, for example.

In order to demonstrate the benefit of a more dynamic response of the working distance $d(t)$, we introduce an additional platform that permits varying the distance between the build surface and the nozzle in z-direction at high velocities and accelerations (see Figure 4). The particular platform used in our laboratory setup is a pantograph, which is connected to a real-time control PC that generates the control input $u(t)$. Accelerations of up to 3m/s^2 can be achieved with this setup in z-direction. We stress the pantograph is only used as a retrofit to an existing machine that is not capable of sufficiently high accelerations. We identify the dynamic behaviour of the platform, i.e., the transfer function G_d, from step responses. Figure 5 shows the average of three measured step responses and the corresponding step response of the transfer function

$$G_d(s) = \frac{1}{1.44 \cdot 10^{-4} s^2 + 1.69 \cdot 10^{-2} s + 1} \tag{2}$$

that resulted from the identification. The distance of the powder nozzle to the build surface is measured by laser triangulation at a frequency of 100 Hz. The pantograph carries out the step in about 50 ms. A lower bound on the distance of the nozzle to the melt pool must be enforced to protect the nozzle from damage by overheating. The minimum distance, including a safety margin, amounts to 6mm in our laboratory setup. The steps shown in Figures 5 and 6 are carried out between the nomimal distance of 8mm and the minimum distance of 6mm.

We claim feedback control is not required for the pantograph, since it is sufficiently accurate under open-loop control for our purposes. This can be seen in Fig. 6, which shows three 2 mm steps performed in quick succession. A homing procedure is performed to reset the working distance to 8 mm after every step.

2.2 Effect of velocity on weld bead height ($G_{\tilde{h}}$)

Figure 7 illustrates the effect of the scanning velocity on the weld bead height for two steps between 5mm/s and 7.5mm/s. We stress the velocities of interest are

those parallel to the build surface now, while Section 2.1 addressed the velocity orthogonal to the build surface.

Note that all parameters, including the values for the nozzle velocity, correspond to typical values of the machine. We claim without giving details that the data for $\tilde{h}(x)$ and $v(x)$ can be transformed into the time-series $\tilde{h}(t)$ and $v(t)$, since the velocity of the nozzle is known from Figure 7c. The resulting time-series for $\tilde{h}(t)$ is shown in Figure 9.

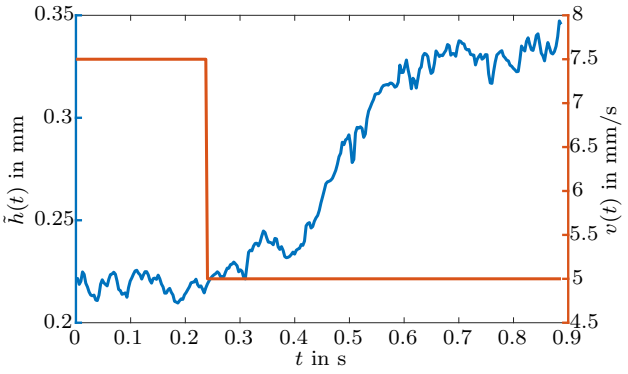

Fig. 8. Average of two recorded step responses of $\tilde{h}(t)$ and the corresponding system input $v(t)$.

We identify $G_{\tilde{h}}$ from the average of the two step responses displayed in Figure 7b. Both $v(t)$ and $\tilde{h}(t)$ of the second step are inverted to match the direction of the first step and the average of both steps is used for simplicity. The finite extension of the melt pool is compensated for by shifting the time series accordingly. The resulting average step used for the identification of $G_{\tilde{h}}$ is displayed in Figure 8. The identification yields

$$G_{\tilde{h}}(s) = -\frac{4.65 \cdot 10^{-2} \cdot e^{-0.0752s}}{3.59 \cdot 10^{-4}s^3 + 1.06 \cdot 10^{-2}s^2 + 0.179s + 1}. \quad (3)$$

We note for completeness that the average value of $\tilde{h}(t)$ before the step, i.e., for $v_0(t) = 7.5$mm, amounts to $\tilde{h}_0 = 0.218$mm.

Figure 9 compares the step response of the transfer function (3) to the original data. It is evident that the weld bead height from Figure 7 is reproduced sufficiently accurately.

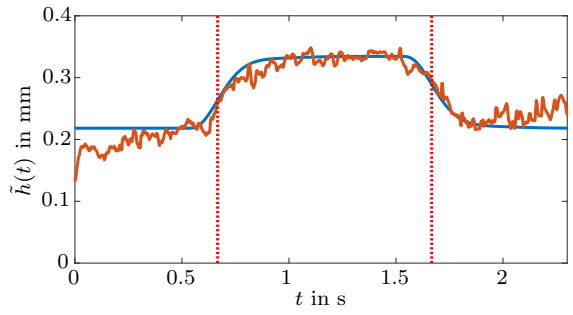

Fig. 9. Actual (red) and simulated (blue) weld bead height $\tilde{h}(t)$. Dotted lines correspond to those in Figure 7.

2.3 Effect of the working distance on weld bead height (K_d)

The working distance $d(t)$ is typically set to the distance of the powder focus to the nozzle (8mm for our laboratory setup). Obviously, at this working distance the highest deposition rates are achieved, since the position of the powder stream with the highest powder density coincides with the melt pool that is created on the build surface. By changing the working distance $d(t)$ and moving the melt pool out of the powder focus, the mass flow rate of powder into the melt pool is reduced. As a consequence, the actual weld bead height $h(t)$ results from the largest achievable one $\tilde{h}(t)$. This reduction can be described with $k(t)$ as introduced in (1). We call $k(t)$ the *efficiency factor*.

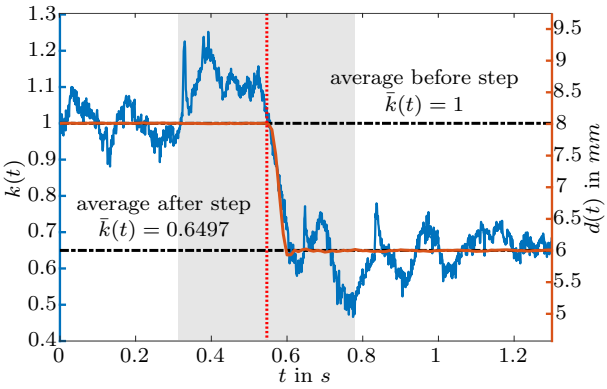

Fig. 10. Response of the efficiency factor $k(t)$ (blue) to a step in the working distance $d(t)$ (red). Dot-dashed lines mark the the average of $\bar{k}(t)$ before and after the step. The shaded time interval was ignored to account for the finite size of the melt pool.

We determine the input-output behaviour from the working distance $d(t)$ to the efficiency factor $k(t)$ with the response shown in Figure 10. The weld bead height $h(t)$ shown in Figure 10 is measured with the same confocal laser scanning device already used in Section 2.2. The time series $d(t)$ shown in Figure 10 and used in the identification is the average from Figure 5.

When averaging $k(t)$ before and after the step in $d(t)$ in Figure 10, it becomes evident that the $k(t)$ follows $d(t)$

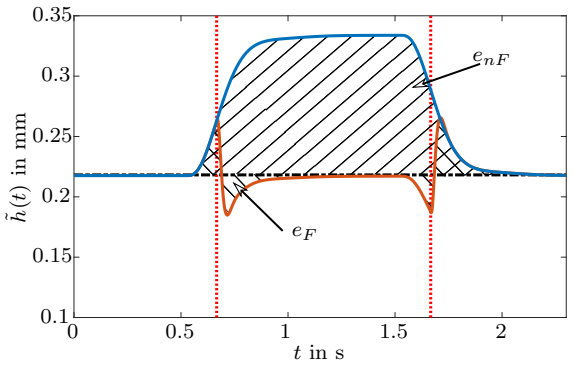

Fig. 11. Simulation of the weld bead height with (red) and without (blue) feedforward control. The hatched areas correspond to the integral errors.

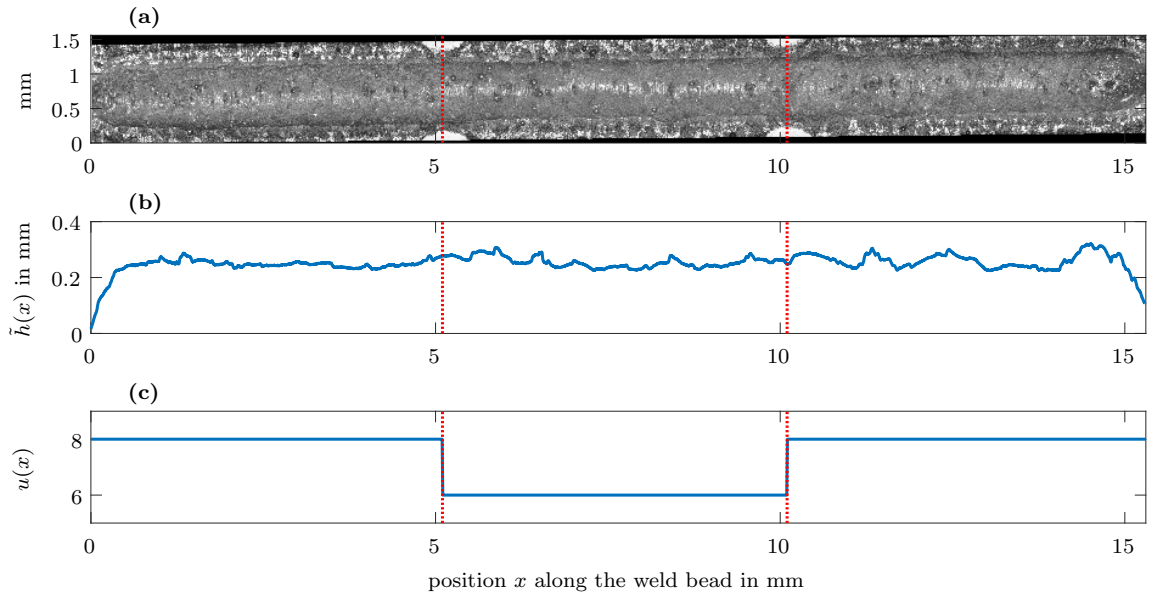

Fig. 12. Weld bead height that results with feedforward control. All parameters are as in Figure 7; in particular $v(x)$, which is not repeated here, changes as in Figure 7. Part (c) shows the signal that results from feedforward control with the model from Figure 3 and the transfer functions from Section 2.

almost instantaneously, which implies a static model is appropriate. More precisely, the static function

$$k(t) = 0.1751 \cdot d(t) - 0.4011 \tag{4}$$

results.

2.4 Structure and simulation of the feedforward controller

After completing the dynamic model sketched in Figure 3 by identifying G_d, K_d and $G_{\tilde{h}}$, we use the model for feedforward control. It is the purpose of this controller to ensure a constant weld bead height $h(t)$ in spite of variations of the nozzle velocity $v(t)$. This is achieved by adjusting $u(t)$ and thus the working distance $d(t)$ and the actual height $h(t)$. Before evaluating the feedforward controller with a test on the laboratory setup in Section 3, we analyse its properties with a simulation. Note that $v(t)$ is available beforehand in the present section and Section 3. The proposed feedforward controller also applies, however, if $v(t)$ is not known beforehand but measured online.

Figure 11 shows $h(t)$ with and without feedforward control for non-constant $v(t)$. The velocity is subject to the same variations as shown in Figure 7. The red vertical lines in the figure mark the points in time at which the steps in $v(t)$ occur. If $u(t)$ is kept constant, i.e., no feedforward control applies, the height increases for decreased $v(t)$ as expected. If $u(t)$ is adjusted to compensate for the change in $v(t)$, the height $h(t)$ can be corrected. Note that the positive and negative integrated errors e_F shown in Figure 11 are approximately equal in size. This indicates the correction for the finite extension of the melt pool is carried out correctly.

The integrated errors shown in Figure 11 amount to $e_F = 0.015$ and $e_{nF} = 0.114$. This corresponds to a reduction by 87% due to feedforward control.

3. APPLICATION TO A DED PROCESS

We implemented the proposed feedforward controller on a DED laboratory setup with the parameters listed in Table 1. Figure 12 shows the weld bead that results for the same conditions as in Figure 7 but with feedforward control.

Table 1. Parameters of the laboratory DED-machine

laser type	diode-pumped fibre laser
wavelength	1070nm
max. laser power	450W
powder nozzle type	coaxial
powder material	316 L stainless steel
build surface material	316 L stainless steel
nominal working distance d	8mm
min. working distance d	6mm

We calculated $u(t)$ that is required to compensate for the variations $v(x)$ shown in Figure 7 (which also apply in Figure 12 but are not repeated there) with the model (3). The resulting $u(t)$ shown in Figure 12c after conversion to $u(x)$ for ease of interpretation.

It is evident from the comparison of Figure 12b to Figure 7b that the error in $\tilde{h}(x)$ can be reduced. Figure 13 shows a quatitative comparison. The resulting control error for the measured height profiles is $e_{nF,m} = 0.1431$ without feedforward controller and $e_{F,m} = 0.0439$ with feedforward controller. The reduction is smaller than in the simulation in Section 2.4. However, it amounts to 69% and therefore is still considerable.

4. CONCLUSION

We proposed a new feedforward controller for the control of the weld bead height for a DED additive manufacturing

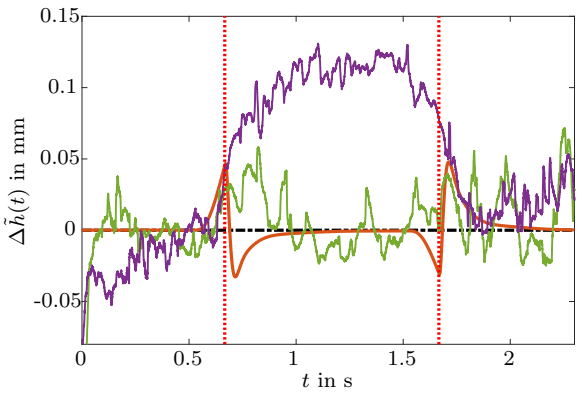

Fig. 13. Deviation $\Delta\tilde{h}(t) = \tilde{h}(t) - \tilde{h}_0$ of weld bead height from setpoint $\tilde{h}_0$ with an without feedforward control. Simulation results with feedforward are shown in red, measured results with and without feedforward are shown in green and purple, respectively. Set points were $\tilde{h}_0 = 0.249$mm and $\tilde{h}_0 = 0.218$mm for the case with and without feedforward control, respectively.

process. The proposed controller is new in that it uses the working distance, i.e., the distance of the processing head to the build surface, as a manipulated variable. We showed that the new controller and manipulated variable can be used to compensate deviations from the desired weld bead height that result from a varying processing head velocity.

Future work will focus on combining feedforward with feedback control and on extending the proposed model for a more systematic treatment of the finite weld bead size. Moreover, we intend to investigate the influence of other parameters, such as laser power and velocity of the processing head.

ACKNOWLEDGEMENTS

We gratefully acknowledge funding by the German Federal Ministry of Education and Research under grant 13N14305.

REFERENCES

Corbin, D.J., Nassar, A.R., Reutzel, E.W., Beese, A.M., and Kistler, N.A. (2017). Effect of directed energy deposition processing parameters on laser deposited inconel® 718: External morphology. *J. Laser Appl*, 29(2).

De Oliveira, U., Ocelik, V., and De Hosson, J.T.M. (2005). Analysis of coaxial laser cladding processing conditions. *Surface and Coatings Technology*, 197(2-3), 127–136.

Devesse, W., De Baere, D., and Guillaume, P. (2014). Design of a model-based controller with temperature feedback for laser cladding. *Physics Procedia*, 56, 211–219.

Dillkötter, D. and Mönnigmann, M. (2019). Design of a model based feedforward controller for additive manufacturing by laser metal deposition. In *2019 18th European Control Conference (ECC)*, 3842–3847. IEEE.

El Cheikh, H., Courant, B., Branchu, S., Hascoet, J.Y., and Guillén, R. (2012). Analysis and prediction of single laser tracks geometrical characteristics in coaxial laser cladding process. *Optics and Lasers in Engineering*, 50(3), 413–422.

Fathi, A., Khajepour, A., Toyserkani, E., and Durali, M. (2007). Clad height control in laser solid freeform fabrication using a feedforward pid controller. *The International Journal of Advanced Manufacturing Technology*, 35(3-4), 280–292.

Haley, J.C., Zheng, B., Bertoli, U.S., Dupuy, A.D., Schoenung, J.M., and Lavernia, E.J. (2019). Working distance passive stability in laser directed energy deposition additive manufacturing. *Materials & Design*, 161, 86–94.

Tang, L., Ruan, J., Landers, R.G., and Liou, F. (2008). Variable powder flow rate control in laser metal deposition processes. *Journal of Manufacturing Science and Engineering*, 130(4), 041016.